WILEY **WIREs** ENERGY AND ENVIRONMENT

OVERVIEW

Addressing the risks of induced seismicity in subsurface energy operations

Richard T.J. Porter[1] | Alberto Striolo[1] | Haroun Mahgerefteh[1] | Joanna Faure Walker[2]

[1]Department of Chemical Engineering, University College London, London, UK

[2]Institute for Risk and Disaster Reduction, University College London, London, UK

Correspondence
Richard T.J. Porter, Department of Chemical Engineering, University College London, London WC1E 6BT, UK.
Email: r.t.j.porter@ucl.ac.uk

Shale gas could help address the insatiable global demand for energy. However, in addition to risks of environmental pollution, the risk of induced seismicity during the hydraulic fracturing process is often considered as the major showstopper in the public acceptability of shale gas as an alternative source of fossil fuel. Other types of subsurface energy development have also demonstrated similar induced seismicity risks. This article presents an interdisciplinary review of notable cases of suspected induced seismicity relating to subsurface energy operations, covering operations for hydraulic fracturing, wastewater injection, conventional gas extraction, enhanced geothermal systems and water impoundment. Possible causal mechanisms of induced seismicity are described and illustrated, then methods to mitigate induced seismicity, encompassing regulations, including so-called traffic light systems, monitoring and assessment, and numerical modeling approaches for predicting the occurrence of induced seismicity are outlined. Issues relating to public perception of energy technologies in regards to induced seismicity potential are also discussed.

This article is categorized under:
    Photovoltaics > Climate and Environment
    Fossil Fuels > Climate and Environment
    Energy Infrastructure > Economics and Policy
    Energy and Development > Systems and Infrastructure

KEYWORDS
hydraulic fracturing, induced seismicity, reservoir injection

1 | INTRODUCTION

Hydraulic fracturing combined with horizontal drilling has stimulated tremendous oil and gas production from shale rock formations in North America. Speculation has mounted as to whether the successes of the shale gas story could be replicated elsewhere, like in Europe where sizeable reserves are known to exist. However, environmental concerns, combined with low oil & gas prices, have tamed this prospect. Different European countries have adopted varying policies towards shale gas, with initial exploration underway in a number of countries such as Poland and England but other countries having banned hydraulic fracturing altogether. Significant technological hurdles remain for the adaptation of hydraulic fracturing techniques to European shales, but a greater challenge for uptake of the technology in Europe is very likely to be achieving "social licence to operate", where the situation in Europe is considerably different to North America. In Europe, there are densely populated regions that are unaccustomed to onshore oil & gas activities, sociological and risk perception differences and hence the same

methods used to solve the problem of induced seismicity in North America may not be applicable. Supporters of this resource point out that natural gas could provide a bridge to decarbonization by facilitating a move away from higher carbon intensity fossil fuels such as coal. However, opponents highlight environmental risks associated with shale gas production such as induced seismicity.

A number of previous review articles have addressed induced seismicity for a range of industrial activities. McGarr, Simpson, and Seeber (2002) provided a general overview of induced seismicity from a range of human activities and discussed the different causal mechanisms. Klose (2010) provided an overview of global statistics of human induced earthquakes and Davies, Foulger, Bindley, and Styles (2013) provided a review of such 198 ≥ 1 magnitude events and then focussed discussion on seismicity induced by hydraulic fracturing. Expanding on these, Foulger, Wilson, Gluyas, Julian, and Davies (2018) produced the most comprehensive review and database containing over 700 cases of anthropogenic projects postulated to have induced earthquake activity. Grigoli et al. (2017) reviewed issues relating to monitoring discrimination and management of induced seismicity in Europe and related case studies. Keranen and Weingarten (2018) reviewed induced earthquakes during the past 10 years related to fluid injection in petroleum fields. The number of documented cases of induced seismicity is rapidly increasing and there is a need to update reviews. In 2017 alone, there were two record breaking magnitude events in the category of reservoir stimulations. In this article, we provide a general review of a number of induced seismicity case studies that have occurred in the last 15 years and that were caused by different industrial activities including subsurface energy operations and the associated possible causal mechanisms. Issues relating to public perception are discussed and we then conclude by highlighting procedures and strategies that could be implemented to help prevent and mitigate future occurrences.

2 | SEISMIC SCALES

Characterizing the strength and effects of seismic events (earthquakes) is important for both naturally occurring and anthropogenic seismicity. Seismic scales characterize earthquake strength either through the intensity of ground shaking, the damage invoked, or by defining magnitude based on measured physical parameters. The observable damaging effects of an earthquake are quantified using intensity scales like the Modified Mercalli Intensity (MMI) scale. Magnitude scales give a measure of the energy released by an earthquake at its source and include the body-wave magnitude (M_b), surface wave magnitude (M_s) and local magnitude (M_L) which use logarithmic formulas based on the amplitude of the earthquake waves at a designated frequency recorded on a seismograph, corrected for the distance from the source and the instrument response. The "Richter magnitude," popular in the media, is another example of a local magnitude scale but it has a drawback of saturation at high magnitudes, meaning that larger ranges of actual earthquake size converge on a narrow range of magnitude values. For example earthquakes with magnitude M_L above 7 are difficult to distinguish using the Richter magnitude scale due to the difficulty in measuring short high frequency waves (Howell Jr, 1981). Alternatively, scientists use the moment magnitude scale (M_w), which is derived from the seismic moment, M_0, a value based on physical properties of the rocks and fault slip. The seismic moment is scaled with a logarithmic formula to yield moment magnitude with values comparable with local magnitude scales, but with the advantage that the M_w scale does not saturate. Accurate magnitude estimation is fundamentally important for the monitoring of induced seismicity in subsurface operations. The determination of magnitude is a challenging process with different induced seismicity earthquake catalogues showing variation depending on the approach used (Edwards & Douglas, 2014). Some emerging approaches for more accurate magnitude estimates for induced seismicity are introduced in the Monitoring and Assessment section below.

For calculating risk and informing building codes, the seismic hazard needs to be determined. A general definition of seismic hazard is the frequency or probability that the ground-motion amplitude exceeds a certain threshold at a specific site (Suckale & Grünthal, 2009). Ground motion is typically measured using PGA (peak ground acceleration) or PGV (peak ground velocity). PGA is the maximum ground acceleration experienced at particular location during an earthquake. Accelerometers are used to record PGA at seismic stations expressed in units of % of acceleration due to Earth's Gravity (g) or m/s². Earthquake ground motion can be in all directions so PGA is often split into vertical and horizontal components with horizontal PGA generally being larger. PGV gives a measure of the maximum speed of the ground at a specific location. PGV is derived from the peak of the first integration of an acceleration record and can be expressed in cm/s.

It should be borne in mind that the effects of a seismic event of a given magnitude in a given location depend heavily on a number of factors that include the duration of the shaking, the distance from the source, depth of the hypocentre, terrain characteristics and earthquake resistance of local structures (Banks, 2006). Equivalence between the MMI scale and any magnitude scale is therefore, at best, an approximation. In particular, hypocentre depths for induced seismicity are often significantly shallower compared to those of natural earthquakes. In fluid injection operations for example, hypocentre locations are much closer to the injection depth, meaning that depth can be a key parameter in discriminating between natural and induced seismicity (Zhang et al., 2016). Hence, induced seismicity of a given magnitude can be more damaging compared to equivalent

magnitude natural seismicity. This has implications for public risk perception because earthquake magnitude is the preferred (and often only) parameter reported by the media after an earthquake leading the general public to perceive a lower severity for a given magnitude than implied by the induced earthquakes' depths. Despite the difficulties of correlating scales, attempts have been made to find regression relationship between MMI and either PGA or PGV. For example, the United States Geological Survey (USGS) compared the peak ground motions to observed intensities for eight significant earthquakes in California (Wald, Quitoriano, Heaton, & Kanamori, 1999; Wald, Worden, Quitoriano, & Pankow, 2005). They found that there was a stronger regression relationship between PGA and MMI than PGV and MMI for lower intensities (MMI < VII), with the opposite for higher intensities (MMI > VIII).

3 | CASES OF SUSPECTED INDUCED AND TRIGGERED SEISMICITY

Several industrial sectors are capable of inducing or triggering seismicity, including mining, water impoundment, conventional oil and gas operations, groundwater extraction, CO_2 Capture and Storage (CCS), waste fluid injections, stimulation of geothermal reservoirs and hydraulic fracturing for shale gas production. Different definitions that make a distinction between induced and triggered seismicity have been put forward. Some authors describe induced seismicity as events with stress change comparable to ambient shear stress that acts on a fault causing it to slip, while triggered seismicity is described by stress changes that are only a small fraction of the ambient stress (McGarr et al., 2002). Other authors describe triggered seismicity as human activity causing events that would have occurred naturally but later in time, while induced seismicity are events that would not have occurred naturally (Cesca, Dost, & Oth, 2013). However, such definitions are not universal. Suspected cases of induced seismicity have been documented as early as the 1930s. For earthquakes with reported magnitude ≥1.5 as detailed in the Human-Induced Earthquake Database (http://inducedearthquakes.org/), mining has contributed to the most number of reported induced seismic events (169), followed closely by water impoundment (158) and then conventional oil and gas operations (88). Waste fluid injections and enhanced geothermal operations are both reported to have induced 43 seismic events with reported magnitude ≥1.5. Hydraulic fracturing for shale gas production has been linked to 37 induced seismic events with reported magnitude ≥1.5, whereas CCS and coal bed methane operations have been linked to one each, although for the latter, strong evidence has been provided that the earthquake was of natural origin (Albano et al., 2017). Figure 1 summarizes some recent induced seismic events linked to industrial activities at various locations across the globe, along with the corresponding approximate magnitude in the scale they have been reported in. We review some of these events in the following sections to demonstrate the different technical experiences and public perception issues encountered with such systems. While
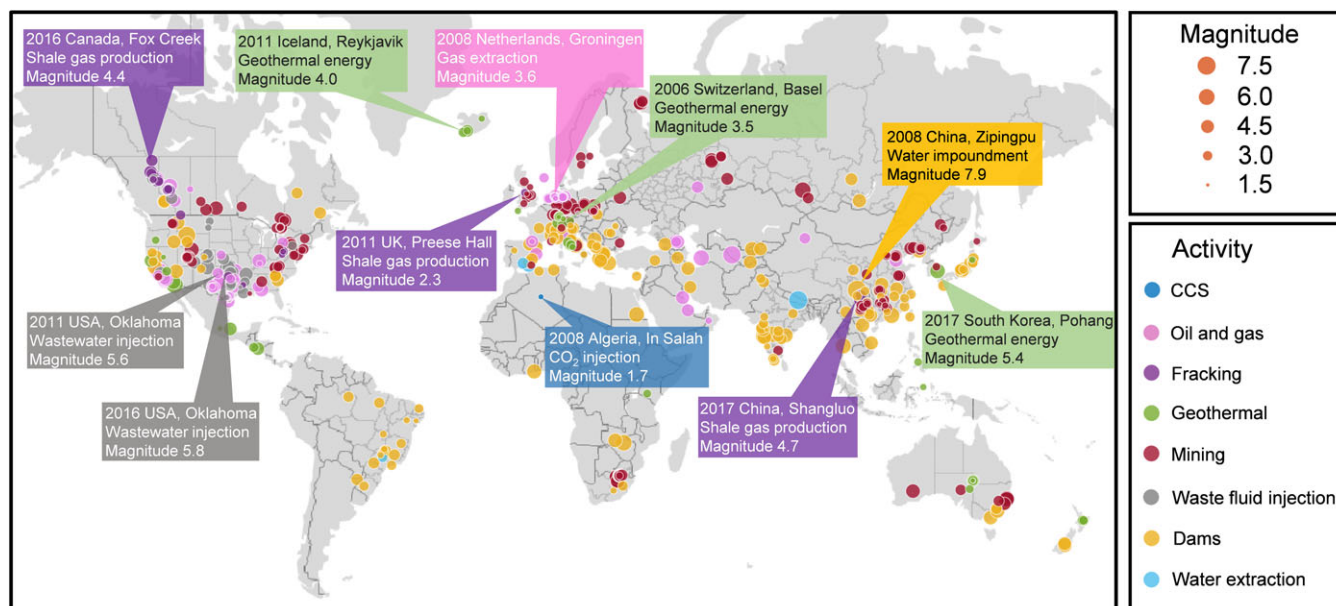

FIGURE 1 Worldwide induced and triggered seismic events with recorded magnitude ≥1.5 that have been linked to industrial activities. The catalogue (source: http://inducedearthquakes.org/) was updated to include the highest magnitude event recorded at the Pohang geothermal site in South Korea (Grigoli et al., 2018). Several categories were omitted, namely construction, deep penetrating bombs, nuclear explosions, research and coal bed methane. Categories of oil and gas and conventional oil and gas were merged, and oil and gas/waste fluid injection was merged with waste fluid disposal to form the category waste fluid injection. The HiQuake database (Foulger et al., 2018) includes all earthquake sequences proposed on scientific grounds to have been human-induced regardless of credibility

some cases that relate to more conventional activities are discussed, the focus here is mainly on subsurface fluid injections during the last 15 years due to the rapid expansion of this industrial activity and its associated increase in induced seismicity. For further discussions on some of the events shown in Figure 1 and other industrial activities, we refer the interested reader to Grigoli et al. (2017), McGarr et al. (2002), Foulger et al. (2018) and Keranen and Weingarten (2018).

3.1 | 2008 Sichuan earthquake, water impoundment

Possibly the largest earthquake suspected to have been triggered by anthropogenic activity occurred in Sichuan, Central China on the 12 May, 2008. Measuring 7.9 on the moment magnitude scale, it was one of the most devastating earthquakes in recent memory with over 80,000 people killed or missing, and half a million people made homeless. Since the earthquake, hundreds of scientific articles have investigated its link to the Zipingpu Dam Reservoir. While many believe that the dam contributed to the triggering of the earthquake, the scientific debate focusses on the precise causal mechanism (Tao, Masterlark, Shen, & Ronchin, 2015). It has been suggested that mass loading of water and its penetration into rock affected the subsurface pressure in an underlying fault line, possibly setting off a series of ruptures that led to the earthquake (Ge, Liu, Lu, Godt, & Luo, 2009). Others have argued that given the conditions, at a depth of 14–19 km, the earthquake was too deep to have been caused by the Zipingpu Dam reservoir (Deng et al., 2010).

3.2 | 2012 Groningen, natural gas production

Onshore natural gas production in the Groningen gas field in the Netherlands began in the 1960s. Gas production in the area has since reduced the subsurface pressure, leading to subsidence and seismicity (van Thienen-Visser & Breunese, 2015). A marked increase in seismicity in the region has been recorded since the 1990s with the largest magnitude earthquake, $M_L = 3.6$, occurring on August 16, 2012. Although the magnitudes of the seismic events have been modest, their shallow depths and the area's soft soils have led to damage to houses and infrastructure. The shaking and damage led to, press interest, widespread public anxiety and a large amount of public turmoil. Public annoyance has also focussed on damage handling and compensation (Muntendam-Bos, Roest, & de Waal, 2017) while property values have tended to fall (Vlek, 2018). To mitigate the risks, the Dutch government has proposed to cap gas production at 12 billion m^3/year by October 2022 with the aim of ending production by 2030.

3.3 | 2006 Basel, enhanced geothermal system

One of the first commercial ventures for an enhanced geothermal system (EGS) was the Deep Heat Mining Project, initiated in Basel, Switzerland in 1996. In EGS, high-pressure water is injected into hot low permeability rock so that heat may be extracted by water recirculation to and from the subsurface. The process is a reservoir stimulation technique that shares many similarities with hydraulic fracturing. In October 2006, the injection well near Basel reached its final depth of 5 km. An array of six down-hole seismic sensors with depths between 317 and 2,740 m was installed and up to 30 surface seismic stations were deployed in the area (Bachmann, Wiemer, Goertz-Allman, & Woessner, 2012). Approximately 11,500 m^3 of high-pressure water was injected between the 2 and 8 of December 2006. This case study provided a large earthquake catalogue. During the 6-day stimulation, around 13,000 induced micro-seismic events ($M_L \geq -1$) were detected by the borehole network. Out of these events, approximately 3,500 were locatable (Häring, Schanz, Ladner, & Dyer, 2008). These events had a range of moment magnitudes M_w 0.1 to 3.2 (Bachmann et al., 2012). When levels of surface seismic activity began to strongly increase on December 8, 2006, the injection was stopped. Some hours later, an M_L 3.4 seismic event occurred. Basel residents described a loud bang and a short period of high frequency shaking. Overall, 28 events with M_L between 1.7 and 3.4 were reported. Slight nonstructural damage, such as fine cracks in plaster was reported. These events provoked outrage among the public and politicians and received intensive media coverage (Wallquist, Visschers, & Siegrist, 2009). Residents' concerns were raised not only for damage from single events but also for the effect of seismicity over the many years of operation of the project (Majer et al., 2007). The public reaction to the nuisance and fear evoked by the felt seismicity led to the suspension of the EGS project (Giardini, 2009; Gischig & Wiemer, 2013). The demonstration of a computational modeling approach applied to the catalogue of fluid-induced seismicity recorded in Basel is shown later in this article.

3.4 | 2017, Pohang, enhanced geothermal system

The first large scale stimulation to establish an EGS in South Korea, conducted at a depth of 4,348 m, began at the Pohang site on January 29, 2016 (Park et al., 2017). The stimulation was carried out in four phases up until September 2017 and involved the injection of a total volume of 12,800 m^3 of water at rates of 1–48.63 L/s (Kim et al., 2018). Wary of induced seismicity that had occurred in other stimulations, the injection procedure had been designed to limit the onset of earthquakes. South

Korea is a relatively quiescent area for natural seismicity compared to neighboring countries. Nevertheless, in September 2016, the largest ever recorded earthquake of natural origin in the country occurred at a depth of 14 km at Gyeongju, measuring 5.8 M_L. Subsequent to the third injection phase on April 15, 2017, a 3.1 M_L earthquake struck near to the well bottom at the EGS site (Grigoli et al., 2018). On November 15, 2017, a 5.4 M_w magnitude earthquake occurred at the Pohang EGS site, at a depth of around 4.5 km, and being associated with six foreshocks and 210 aftershocks. This earthquake was the most damaging in South Korea since seismicity records began in 1903, being around 1,000 times stronger than the one that occurred in Basel, injuring 70 people and causing serious damage to the value of $52 million. Although the earthquake reportedly occurred some 2 months after stimulation activities had ceased, researchers believe it likely that the earthquake was caused by the EGS activities, evidenced by the shallow depth of the main seismic events—a key discriminant between natural and induced seismicity. The contribution of the earlier Gyeongju earthquake to triggering the Pohang earthquake has also been studied (Grigoli, Cesca, et al., 2018). The EGS operation was suspended by court order after citizens had filed to stop the operation. The South Korean Energy Ministry began an independent inquiry involving an international team of scientists.

3.5 | 2011–2016, Oklahoma, wastewater disposal

The rate of seismicity in the state of Oklahoma, USA, has risen dramatically since 2009 (Ellsworth, 2013). In 2015 alone, approximately 900 earthquakes with magnitude ≥3 were reported, contrasting to only around 1 per year prior to 2009 (see Figure 2, reproduced from Induced Seismicity, 2017). On September 3, 2016, a 5.8 M_w earthquake struck in Pawnee County, making it the largest earthquake ever to be recorded in Oklahoma. The earthquake caused light to medium damage to buildings in Pawnee City and was felt in at least six neighboring states. The documented huge increase in seismicity is widely attributed to widespread wastewater disposal via thousands of injection wells dotted around the state. Oil extraction in Oklahoma produces saltwater too saline for any use at the surface. The produced water is often injected into oil reservoirs to increase production via water flooding. Injection volumes in North-Central Oklahoma are as large as 200 million m^3 in an area of around 8,000 km^2, with peak injection rates reached in 2015 (Langenbruch & Zoback, 2016). Four high rate injection wells located in southeast Oklahoma City had a combined disposal of 4 million barrels of waste water per month between 2008 and 2014. It is believed that these large injected volumes caused pore pressure increases in the subsurface, leading to a reduction in resistance to sliding on preexisting faults. Public concerns over induced seismicity in Central United States due to both drilling and deep-well injection of waste fluids have received widespread publicity in national and local media (Graham, Rupp, & Schenk, 2015). In May 2016, regulators ordered a 40% reduction in saltwater injection rates. Although some large events greater than M_L 5 have occurred since, there has been a dramatic reduction in seismicity, suggesting the regulation was effective (Petersen et al., 2018).

3.6 | 2009–2016, Western Canada, hydraulic fracturing

Canada is the second largest producer of shale gas in the world after the United States, with much of the shale development focussed in the Western Canada Sedimentary Basin. Low levels of seismicity are expected during hydraulic fracturing, as high-pressure fluids break the rocks causing micro-earthquakes. However, in Western Canada, 3% of hydraulic fracturing operations have been accompanied by seismic events with M_L greater than 3. This was unexpected, given the relatively small
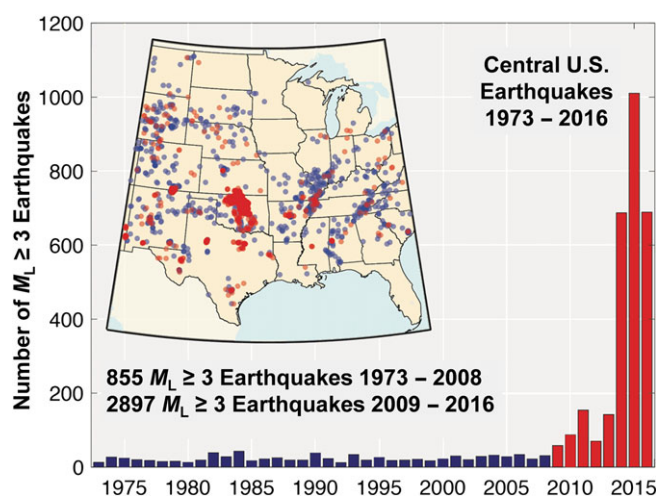

FIGURE 2　Annual number of $M_L \geq 3$ earthquakes in Central United States (the red cluster in the Centre of the map highlights earthquakes in Oklahoma, 2009–2016) reproduced with permission from (induced seismicity, 2017), copyright USGS

volumes of fracturing fluid used (Maxwell, 2013; Schultz, Wang, Gu, Haug, & Atkinson, 2017). The largest earthquake of this kind occurred in Fox Creek, Alberta on the January 12, 2016, with M_L 4.1. Although no damage or injuries were reported, Fox Creek town residents described pictures shaking on walls and the sensation of a large truck passing by (Mertz & Ramsay, 2016). The hydraulic fracturing operation was temporarily suspended to reduce risks, but regulators allowed its resumption some three months after the earthquake.

Researchers investigating induced seismicity observed in Alberta have correlated fluid injection volume with earthquake activity while finding other factors like injection pressure and rate to have an insignificant impact on seismicity (Schultz, Atkinson, Eaton, Gu, & Kao, 2018). An M_L 4.1 event is however much higher than what is predicted by the McGarr relation (McGarr, 2014) which correlates fluid-injection-induced earthquakes to the net volume of injected fluid (Atkinson et al., 2016). This contrasts to findings on the importance of injection rate being significant for the onset of induced seismicity in Central United States (Weingarten, Ge, Godt, Bekins, & Rubinstein, 2015).

3.7 | 2011, Lancashire, hydraulic fracturing

In the United Kingdom, during April and May 2011, hydraulic fracturing tests were carried out in the Bowland Shale region at the Preese Hall site in Lancashire, near Blackpool. On April 1, an M_L 2.3 earthquake occurred, followed by an M_L 1.7 event on May 27 (Clarke, Eisner, Styles, & Turner, 2014). The oil and gas exploration and production company Cuadrilla suspended the operation and commissioned a series of studies to investigate the cause of the seismic events (de Pater & Baisch, 2011). The U.K. government subsequently imposed a moratorium on further activities and commissioned independent reports. The April 1st earthquake, which occurred 10 hours after fluid injection had stopped, was believed to have been caused by fluid penetrating into a nearby, previously unidentified, pre-stressed fault zone, with the fluid pressure reducing the effective stress on the fault, allowing it to slip (Green, Styles, & Baptie, 2012). A fault suspected of being responsible for the earthquakes was later revealed by a 3D seismic survey (Clarke et al., 2014). The U.K. government lifted the moratorium in December, 2012 to allow shale gas exploration activities to resume under stricter controls (Davey, 2012). In August 2013, Cuadrilla drilled an exploratory borehole at Balcombe, West Sussex, United Kingdom. Protests against hydraulic fracturing for shale gas development that took place at the drilling site between July and September 2013 were widely publicized (Andersson-Hudson, Knight, & Humphrey, 2016).

3.8 | 2017, Sichuan Basin, hydraulic fracturing

China is considered to have the world's largest technically recoverable shale gas reserves (EIA & ARI, 2013). The shale gas industry in China is relatively new and concentrated in the Sichuan Basin, itself situated at the eastern edge of a major earthquake prone region marking the boundary with Tibetan Plateau where widespread seismicity has occurred due to the collision between the Indian and Eurasian tectonic plates and is the location of the 2008 earthquake described above. China's shale gas lies in deep and geologically complex formations, which makes it more technically difficult to extract than elsewhere. It has been pointed out that environmental protection regulation lacks specificity for shale gas development in China (Li, Zhou, & Li, 2013). At the Shangluo shale gas site, hydraulic fracturing of previously horizontally drilled wells began in 2014 (Lei et al., 2017). The "zipper" fracturing technique, where 2 or 3 wells are fractured side by side with staggered injection stages, was used at depths of 2.3 to 3 km. Since December 2014, the area has experienced a dramatic increase in seismicity, with more than 2,400 events with magnitude M_L > 1.0 and four M_w > 4.0. The 13 largest events (M_w > 3.5) occurred at depths ranging from 1.8 to 4 km, with most of these events located in the upper parts of the underlying formation beneath the shale formation that was hydraulically fractured. The largest M_w 4.7 event at a very shallow depth of 1.8 km caused heavy damage to a nearby village, with 23 collapsed and another 548 badly damaged houses. This event is likely to be the largest and most damaging earthquake ever to be triggered by hydraulic fracturing (Lei et al., 2017), exceeding the previous highest record in Western Canada. Researchers observed that earthquake magnitudes associated with hydraulic fracturing operations in the Sichuan basin are significantly higher than those in United States, United Kingdom, and Canada. This might be due to the high strength of the hard Pre-Triassic sedimentary rocks that allow high levels of stress in the reservoir to be maintained before failure through brittle fracturing during seismic fracturing.

4 | PUBLIC PERCEPTION

The sample case studies described above have demonstrated that negative public perception to induced seismicity is a potential hazard for subsurface energy operations with numerous international projects having been suspended, delayed or curtailed because of local public opposition. Surveys have shown declining support for shale gas development among the U.K. public

and considerable concern over the possible link between hydraulic fracturing and earthquakes (O'Hara, Humphrey, Andersson-Hudson, & KnightPublic, 2015). Shale gas exploration has been banned in Scotland but is continuing in England amidst opposition and protests. The Groningen case study, representative of a conventional operation, has highlighted that induced seismicity is a major concern in the Netherlands. Although conventional and unconventional gas extraction techniques are quite different, the social impacts relating to fear and anxiety are similar (van der Voort & Vanclay, 2015) and as such, there has been limited shale gas development in the Netherlands due largely to lack of social license to operate (TerHeege, 2016).

It has been reported that both the public and policy makers hold misconceptions about induced seismicity (Trutnevyte & Ejderyan, 2017) and these coupled with a lack of knowledge may influence risk and benefit perception of energy technologies. For example, misconceptions about the depths at which subsurface operations take place may arise from schematics which are not drawn to scale. A technically robust, transparent and balanced dialogue between industries, regulators, the public and other stakeholders can help to resolve misconceptions and risk perception. The development of reliable risk assessment and mitigation strategies that embody computational models capable of predicting the conditions of the injection reservoir would be an important component in facilitating this dialogue (Bendall et al., 2012). Well-designed communication campaigns, which are addressed to the general public as well to technical audiences are therefore highly important and very necessary (Grigoli et al., 2017). The U.S. Department of Energy has produced a protocol in the context of geothermal energy development which provides a set of general guidelines for evaluating and managing the effects of induced seismicity. These guidelines suggest an approach to engage public officials, industry, regulators, and the public at large for facilitating the approval process and avoiding project delays (Majer, Nelson, Robertson-Tai, Savy, & Wong, 2011).

How the public perceives the risks of induced seismicity is likely a key factor for the successful development of subsurface energy operations. Only a few studies have been published on public attitudes towards induced seismicity caused by energy developments (McComas, Lu, Keranen, Furtney, & Song, 2016). Among existing studies, work on EGS (Majer et al., 2007) reports that public perception can vary significantly depending on site location. Interestingly, operations in remote and sparsely populated locations generate little associated public anxiety, while sites near densely populated urban areas are more likely to consider induced seismicity as a potential nuisance. The level of natural seismicity at a given location may also have an impact on public perception. On one hand, communities in areas that experience natural seismicity may be unperturbed by low levels of induced seismicity. However, the public may misconstrue that energy operations are responsible for triggering larger natural seismic events.

An important determinant of public acceptability of a given technology is laypeople's risk perception and benefit perception. Local benefits include job creation, royalties and district heating, including heated swimming pools in some cases. However, such incentives may also be perceived as bribes if offered to communities with negative perceptions of a technology. A technology can be perceived to yield global benefits in terms of its environmental sustainability, such as greenhouse gas emissions reduction. It has been observed that some levels of support can be gained if local communities experience direct economic benefits. A recent survey documents that negative perceptions can arise where beneficiaries are deemed to be solely private companies while the public bears the seismicity risk (Majer et al., 2007; McComas et al., 2016). The public may also hold skepticism about claims of benefits, such as hydraulic fracturing leading to a reduction in U.K. gas prices and mistrust about cost savings being passed on to the consumer (Williams, Macnaghten, Davies, & Curtis, 2017). Fairness in how benefits are distributed and procedural fairness in decision-making process are considered to enhance public acceptability in energy technology development. The extent to which the public feel included in the decision making and have their views respected are aspects of procedural fairness (McComas et al., 2016). Transparent risk communication plays an important role: seismologists and earthquake engineers have called for risk management to be performed in partnership with society (Trutnevyte & Ejderyan, 2017). The establishment of a dedicated seismic monitoring system with real-time analysis coupled with clear, transparent decision protocols is advocated, especially in high-population density areas (Grigoli et al., 2017). Making seismicity data publicly accessible via public institutions in as close to real time as possible has also been recommended, although the format chosen to present the data is debated.

5 | MECHANISMS OF INDUCED SEISMICITY

The sample case studies reviewed above and considered in Figure 1, allow us to tentatively link the possible causes of induced seismicity, as schematically depicted in Figure 3. The commonality of these mechanisms is that the stress field in the shallow Earth's crust is altered by the subsurface operation. A general mechanism for induced seismicity by fluid injections is pore pressure increase via pressure diffusion away from the reservoir away from the injection well. This leads to a reduction in the effective normal stress on preexisting faults; allowing frictional resistance to fault sliding to be overcome (panels a and b). This mechanism could potentially occur in wastewater injection into permeable rock formations, as it requires a high
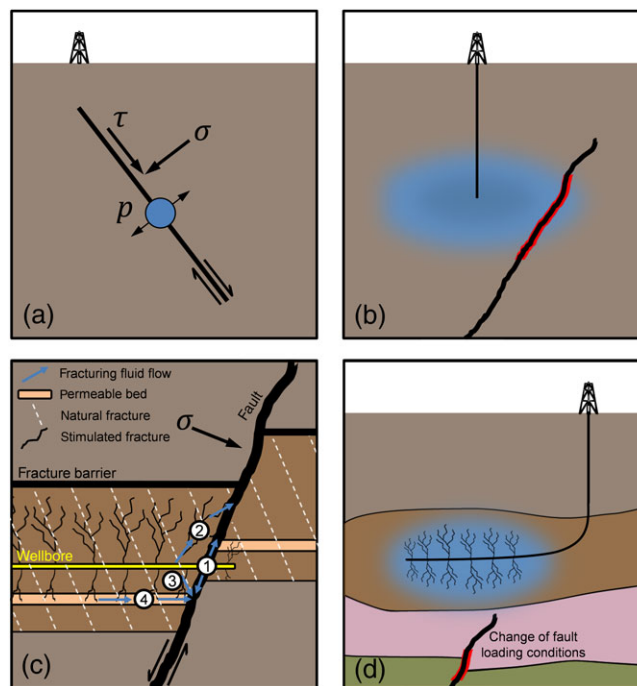
FIGURE 3 Physical mechanisms that could induce seismicity: (a) and (b) pore pressure (p) increase via a diffusional process, leads to a reduction in the effective normal stress (σ) on preexisting faults allowing shear stress (τ) to overcome frictional resistance to fault sliding; (c) in hydraulic fracturing (1) injection well drilled directly into fault, (2) hydraulic fracture directly intersects fault, (3) fluid flow through existing fractures, (4) through more permeable rock strata above or below shale formations, or through bedding planes that interface the rock strata; (d) changes in the stress field brought about by changes in volume or mass loading transmitted to the fault poroelastically (after (Davies et al., 2013; Grigoli et al., 2017; Schultz et al., 2017)

permeable pathway from the fluid injection point to the preexisting fault. The picture is more complex in the case of hydraulic fracturing of low permeability rock formations (panels c and d). Firstly, levels of micro-seismicity that are too weak to be felt at the surface are generated during the creation of fractures in the rocks themselves. These events are part of the hydraulic fracturing process, which induces the formation of fracture networks to enhance fluid transport in the subsurface. Source mechanisms of these small hydraulic fracturing microseismic events are likely to display a volumetric component that has either opening or closing movement in addition to shear slip (Warpinski, Mayerhofer, Agarwal, & Du, 2013). For the triggering of events that are strong enough to be felt at the surface, several scenarios are possible, which could generate a permeable pathway between the fluid injection point and a preexisting fault. Direct fault activation may occur when a hydraulic fracture directly intersects a preexisting fault. Indirect activation could be triggered by diffusion of pore pressure away from the injection zone along local faults and fractures. Additionally, faults may be activated if injection wells are drilled directly into them, via fluid flow through existing fractures, through more permeable rock strata above or below shale formations, or through bedding planes that interface the rock strata (Davies et al., 2013). Even in the circumstances when stimulated fractures and the fracturing fluids may be hydraulically isolated from any preexisting faults, the fault may in fact be activated through perturbations in the stress field brought about by changes in volume or mass loading transmitted to the fault poroelastically (panel d). Such effects can be caused by mass loading on the surface by water impoundment activities.

The orientation of a fault in relation to local stress fields and geological conditions can have a significant influence on the likelihood of slip occurrence. In general, existing faults and fractures are subject to natural horizontal and vertical stresses which act on subsurface rocks. The stress tensor can be described by the vertical stress (σ_2) and the minimum and maximum horizontal stresses (σ_3 and σ_1) that act in two orthogonal directions. In most cases, the Sv is the easiest to estimate since it can simply be found from the weight of the overlying rock. The direction of σ_3, as well as the relative values of σ_1, σ_2, and σ_3, and the fault inclination govern the propensity of fault slip. The normal and shear stresses acting on the fault depend on the orientation of the fault and on the stress state in the rock, as shown in Figure 4 through illustration of the conditions in which a fault is more or less likely to slip. For the two faults illustrated, stimulated by approximately the same horizontal stresses, the fault on the right is more likely to slip. The fault on the left is less likely to slip because the maximum horizontal stress, σ_1, is more perpendicular to the fault. Pore pressure acts equally on all three normal stresses but not on the shear stress (Altmann, 2010). The differential stress, equal to the difference of maximum and minimum principal stresses, remains constant. The reduction of effective normal stress leading to fault sliding can be illustrated by means of a Mohr diagram as shown in Figure 5, which gives a graphical representation of the stress components acting on a fault plane. In a 2D case, the rock's
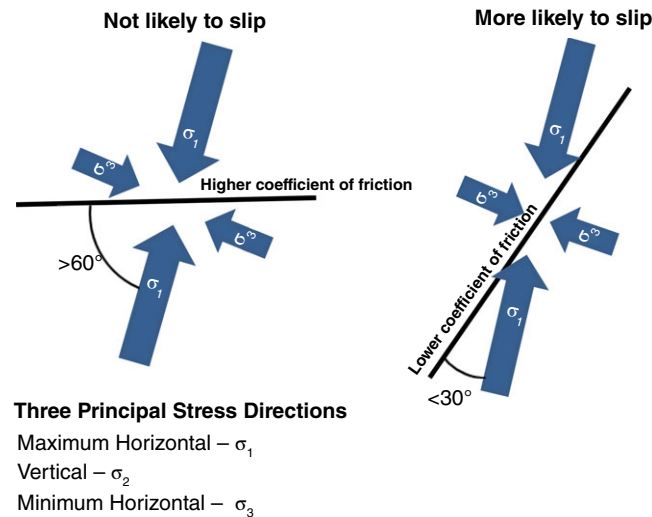
FIGURE 4 Illustration of the relative orientation of stress field and fault direction, with the correspondent expected coefficient of friction and likelihood of slip (after StatesFirst (2015))
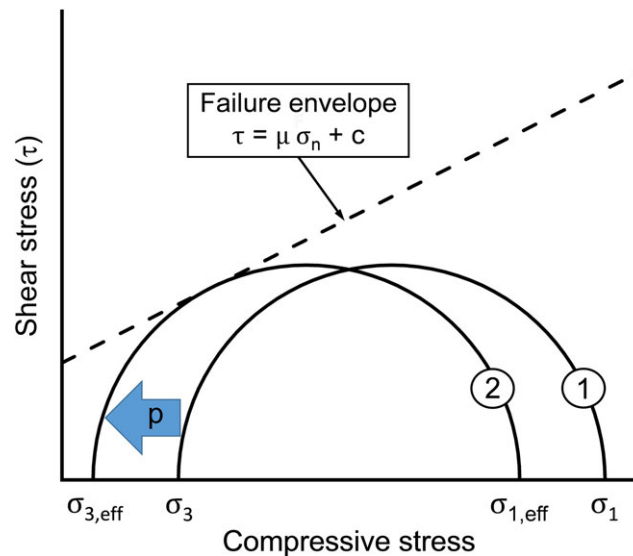

FIGURE 5 A Mohr diagram representation of critical stress state of a fault plane and pore pressure decreasing the effective normal stress. Mohr circle (1) shows the original stress state before pore pressure increase. Pore pressure increase (represented by the blue arrow) leads to a reduction in the compressive stresses, σ_1 and σ_3, so the more circle shifts left to a new position represented by Mohr circle (2). If the failure envelope, shown by the dashed line and controlled by the coefficient of friction μ and cohesion c, is intersected by the Mohr circle then shear failure occurs and a seismic event is induced

stress state is described by the Mohr circle with radius equal to the differential stress and centre point at [½($\sigma_1 + \sigma_3$), 0]. The shear and normal stresses on a fault oriented at the angle θ to the σ_1 direction are determined by the intersection of the radius at angle 2θ with the Mohr circle (Fischer & Guest, 2011). The failure envelope is described by:

$$\tau = \mu\,\sigma_n + c, \tag{1}$$

where μ is the coefficient of friction. Coefficients of friction can be approximated to 0.6 for large effective normal stresses and 0.85 for smaller normal stresses (Byerlee, 1987).The cohesive strength of the rock (cohesion) is denoted by c. If the stress state is initially close to the failure envelope, the fault is termed critically stressed. Natural background seismicity is an indicator of the existence of critically stressed faults (Maxwell, 2013). As pore pressure increases, the reduction of the effective normal stress causes the Mohr circle to shift to the left, but as the shear stress and differential stress remain constant the Mohr circle's diameter is unchanged. The Mohr circle may then intersect the failure envelope and a seismic event is triggered when the shear stress exceeds the failure envelope. The most optimally orientated faults are those at half the angle prescribed by the point at which the Mohr circle is tangential to the failure envelope (Goertz-Allman & Wiemer, 2013).

6 | TRAFFIC LIGHT SYSTEMS

Given the possibility of inducing seismicity via subsurface operations, it is important to minimize the likelihood of occurrence of larger events, and implement robust mitigation strategies. At present, risk mitigation strategies for induced seismicity in fluid injection operations mainly rely on monitoring systems. These so-called Traffic Light Systems were originally proposed by Bommer et al. (2006), and more sophisticated adaptations are based on three independent parameters: (a) public response; (b) local magnitude (M_L); and PGV (see Häring et al., 2008 for further details). TLS deploy a predetermined set of hazard mitigation actions that can vary between locations, regions, countries or types of operation:

- Green: operations and monitoring continue as planned.
- Amber: injection proceeds with caution at possibly reduced volumes and rates.
- Red: injection is stopped. Flowback is possibly initiated.

Although the TLS is widely implemented, the thresholds differ significantly depending on local regulations (see Table 1). For example, TLS for hydraulic fracturing in the Bowland Shale have adopted a cautionary red-level threshold of 0.5 M_L for demanding the cessation of injection and immediate flow-back. This is considerably lower than the limit of 4 M_L in Alberta and British Columbia. According to governmental reports, the limit for U.K. operations may be raised once confidence in the operation has been established (Green et al., 2012). TLS require robust seismic monitoring arrays to be in place before, during and after operations. Additionally, induced seismicity mitigation strategies are enhanced by preliminary screening assessments of seismic risks and faults. During the EGS Basel injection in 2006, a 4-level TLS was used, with operations halted when the red level limit of 2.9 M_L was exceeded.

Although TLS are a relatively simple approach to manage risks associated with induced seismicity, they are not without inherent shortcomings. For example, in the case of the EGS Basel case study discussed above, the implementation of the TLS was unable to mitigate the larger post-injection event with 3.4 M_L. Indeed, some models suggest that shutting in the operation may not always prevent induced seismicity, with, instead, abrupt shut-in possibly leading to locally sharp increases in seismicity (Segall & Lu, 2015). Many fluid-induced seismicity case studies have exhibited maximum magnitude events occurring post shut-in, such as at Preese Hall for example (de Pater & Baisch, 2011).

TLS are considered to be a reactive classification of risk treatment, involving the management and response to a known risk (Kao, Eaton, Atkinson, Maxwell, & Babaie Mahani, 2016), whereby the operations are modified once the thresholds are reached. Current mitigation methods are not predictive in the sense that the thresholds used in the TLS are fixed and not affected by the actual response of the reservoir to injection (Gischig, Wiemer, & Alcolea, 2014). Thresholds are selected on a somewhat ad-hoc basis by experts who determine the risk potential based on the local conditions. Past experience has demonstrated that this approach can sometimes fail to prevent induced seismicity, with large events occurring even after injection has stopped. To operate conservatively, one could select stringently low thresholds in the TLS, but such an approach could significantly constrain the commercial success of a project. It should also be considered that operational or process safety factors may not always allow the implementation of a protocol such as stopping pumping once a threshold has been exceeded; this is often unaccounted for in mitigation strategies (Wiemer, Kraft, Trutnevyte, & Phillipe, 2017). To date, TLS have been used for fluid injections, but the extent to which they can be used for other types of subsurface operation such as gas extraction, which have different spatial and temporal delays is questionable (Bommer, Crowley, & Pinho, 2015). Even the use of magnitude as the basis of most TLS is debated because magnitude is not the best indicator of damage potential when compared to, for example, PGA and PGV. To some extent, the latter quantities could be estimated through the use of mathematical models for predicting ground motion. Adaptive TLS have been proposed to overcome the shortcomings of existing methods. These second-generation methods are predictive, probabilistic, and adaptive in the sense that real time seismicity data is analyzed during operation and thresholds are adjusted based on forecast seismicity risk (Grigoli et al., 2017). The reliability of

TABLE 1 Traffic light systems used to mitigate seismic risk in subsurface fluid injection in different locations

	United Kingdom	Illinois[a]	California	Canada	Basel
🔴	$M_L > 0.5$	$M_L > 4.0$	$M_L > 2.7$	$M_L > 4.0$	$M_L > 2.9$
🟡	$0 < M_L < 0.5$	$2.0 < M_L < 4.0$	–	$2.0 < M_L < 4.0$	$M_L > 2.9$ (orange)
					$M_L > 2.3$ (yellow)
🟢	$M_L < 0$	$M_L < 2.0$	$M_L < 2.7$	$M_L < 2.0$	$M_L < 2.3$

[a] In Illinios, injection wells must cease operations immediately if an identified well receives a third Yellow Light Alert and within the last year the same permittee received a Notice of Violation for the same well related to flow, pressure or mechanical integrity; or if an identified well receives a fifth Yellow Light Alert. If an operator receives three Yellow Light Alerts within a one-year period, they must immediately reduce injection rates and consult with the authorities.

these methods is likely to depend on the reliability of the models used within them. A summary on models currently available to predict induced seismicity is provided below.

7 | MONITORING AND ASSESSMENT

The monitoring and documenting of seismicity associated with subsurface technology is used to assess their characteristics and is also an essential component of TLS. Monitoring systems for induced seismicity consist of arrays of surface or down-hole seismic sensors. They can be used to measure the magnitude and location of seismic events and for determining the extent and direction of the growth of hydraulic fractures (Warpinski, Du, & Zimmer, 2012). Operators select technologies to deploy based on technical challenges, budgets and regulations. Seismic monitoring operations incorporate arrays of geophones or accelerometers. These can be deployed in single or multiple (horizontal or vertical) monitoring wells near the operation, inserted directly into the well being monitored, placed on the surface near wells or buried at shallow depths up to 100 m. Modern arrays can consist of hundreds or thousands of geophones. Seismic resolution is highly site-, survey- and fault-specific (White and Foxall, 2016). Event size and hypocentre location are assessed using algorithms that analyze P-wave and S-wave travel times and waveforms. Seismic events can be monitored in 3D space, and also as a function of time. The accuracy of event location calculations depends on the recording instrumentation and on the velocity model used to compute seismic wave travel times. The characterization of velocity models is therefore crucial to the seismic interpretation (Stork, Verdon, & Kendall, 2014). Challenges for locating and measuring the magnitude of induced seismicity events using seismic monitoring systems include working in high noise environments that often exist around industrial sites, the requirement to detect low magnitude events and the ability to distinguish multiple simultaneous events. Standard methods for earthquake detection use "picking" algorithms that identify changes in the energy and/or frequency of the recorded signals that must be identified by multiple seismic stations within a certain time period (Verdon, Kendall, Hicks, & Hill, 2017). New analysis methods designed specifically for induced seismicity monitoring such as waveform-based analysis (Cesca & Grigoli, 2015; Grigoli, Scarabello, Böse, Weber, & Wiemer, 2018; Pesicek, Child, Artman, & Cieślik, 2014), which use the full waveform recordings as input, present advantages because they can simultaneously detect and locate seismic events and perform well in noisy environments. These can however be computationally intensive and hence may be less suitable for real-time monitoring of operations. The beamforming technique has been developed to enhance detection performance of monitoring induced seismicity while using less expensive and more logistically feasible sparser surface arrays compared to downhole monitoring systems. The design of induced seismicity monitoring infrastructure is highly application-dependent and, importantly, it needs to form part of the overall seismic hazard assessment, in consideration of site characterization and the regional seismic detection networks. For an in-depth discussion of induced seismicity monitoring, the interested reader is referred to Grigoli et al. (2017). Bohnhoff, Malin, ter Heege, Delflandre, and Sicking (2018) provided suggestions for best practice of seismic monitoring and reservoir characterization of unconventional reservoirs, including sensor deployments and depths. A reservoir management plan that integrates the relatively new Seismic Emission Tomography technique for the monitoring scheme is advised as best practice by these authors and a framework for applying cost-effective monitoring strategies using a stepwise approach over reservoir project phases is given. On regional scales, seismic monitoring is typically carried out by geoscientific organizations such as the British Geological Survey, or the TexNet Seismic Monitoring Program in Texas.

In the United Kingdom, operators wishing to undertake hydraulic fracturing operations must submit their plans, which include the seismic monitoring program, to the relevant governmental department and the Environment Agency for approval prior to the operation commencing (EADD, 2014). The plan must include:

- Mapping of faults near the well, an assessment of faulting and formation stresses and risk of fault reactivation.
- Information on the local background seismicity and risk of induced seismicity.
- A summary of the planned operations, including stages, pumping pressures and volumes.
- Measures to mitigate the induced seismicity risk and monitoring of seismicity during the operations.
- Details of the real-time traffic light system and methods of fracture growth monitoring.

If the low level 0.5 M_L red event were triggered, the regulators would explore its implications before deciding whether operations could resume. The regulators would also decide whether any further precautions are necessary to prevent undue risk. Adhering to the regulatory environment enabled by the TLS and other safety measures can promote safe operations accepted by all stakeholders. For example, geothermal operations seem responsible for causing induced seismicity in Iceland. The largest event was an M_L 4.0 earthquake that was felt in Reykjavik (Bessason et al., 2012; Juncu et al., 2018). The operator, Reykjavik Energy, enhanced its public engagement and implemented a new traffic light system. These procedures helped

maintain the social license to operate. The geothermal operations continue today in Iceland in an atmosphere of public acceptance (Urban, 2017).

8 | INDUCED SEISMICITY MODELS

An important prerequisite for the preliminary assessment of the risk and consequences of induced seismicity is the development of robust predictive methodologies based on geological conditions and injection parameters such as volumetric rates and pressures. Devising predictive methodologies for seismic hazard assessment that can encapsulate the complexities encountered in the subsurface, along with a range of possible causal mechanisms of induced seismicity is not without its challenges. Modeling approaches range in complexity from those based on simple empirical observations to complex 2D and 3D mathematical models requiring advanced computational platforms (StatesFirst, 2015). Many approaches to modeling induced seismicity are statistical in nature, being based on correlations of injection rates to observed seismic behavior. Current research aims to develop coupled reservoir and geomechanical models for computer simulation of subsurface fluid injections and fault reactivation given a suitable site characterization (Fault Slip Potential, n.d.). Reservoir models for fluid flow can be used to predict subsurface pressure changes during and after injection. Mathematical models for reservoir simulation first emerged in the 1930s with the first computational software appearing in the 1960s. Analytical solutions have been obtained for different types of reservoir and injection conditions. Numerical models that are based on the solution of sets of finite-difference equations describe transient, multi-phase flow in heterogeneous porous media (StatesFirst, 2015). With a prediction of pore pressure changes from the reservoir model, the potential to induce seismicity can then be assessed using geomechanical models of faults, which can predict their propensity for slip. More recently, models that couple the reservoir fluid flow with the geomechanics behavior have emerged (Rutqvist, 2011).

A seismicity-based reservoir characterization approach has been proposed by Shapiro and Dinske (2009) and is applied to micro-earthquakes that result from subsurface fluid injections. This modeling approach is exemplified here for quantifying induced seismic activity due to fluid injection using the Basel EGS as a case study comprises linked hydrological and geomechanical models. This case study is discussed above in detail. The spatiotemporal evolution of seismicity and the migration of fluids away from the injection point can be illustrated by plotting the observed seismicity as a function of distance and time as in Figure 6 (data from Kraft & Deichmann, 2014).

An approximated hydrological model could predict the transient pore pressure variation as a function of radial distance from the injection point (r) and time (t). It could be set up in a 1D spherical coordinate system as a first approximation. In this model, a diffusional process of relaxation of pore pressure perturbation (p) is adopted. For the case of injection into a homogeneous, poroelastic medium in spherical geometry with azimuthal and poloidal symmetry, the diffusion equation is:

$$\frac{\partial p}{\partial t} = \frac{D}{r^2}\left[\frac{\partial}{\partial r}\left(r^2\frac{\partial p}{\partial r}\right)\right], \tag{2}$$

where D is hydraulic diffusivity in units of m²/s. The diffusion equation is solved here using a numerical approach through the application of an explicit forward differencing scheme in a 1-D physical domain of 952 m length which was selected in suitable excess of the stimulated volume in the Basel case study. 1,201 nodes are used at equally spaced 0.79 m intervals. In the approximated model the reservoir is considered homogeneous and isotropic with hydraulic diffusivity set at 0.05 m²/s at
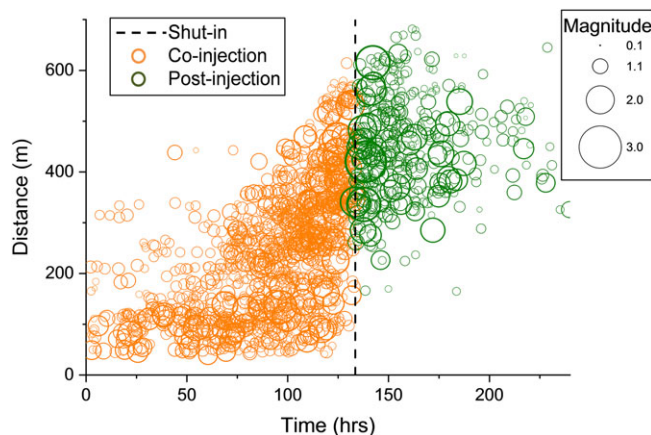

FIGURE 6 Evolution of recorded seismicity during the Basel EGS stimulation as a function of the distance from the well shoe casing versus time (data from Kraft and Deichmann (2014))

all locations. This value is believed to be typical of granites with preexisting fractures (Shapiro, Audigane, & Royer, 1999). An injection pressure at the centre of the sphere with radius $a_0 = 2.38$ m (equivalent area to the open hole section of the Basel injection well) is specified on the first four nodes closest to the sphere origin, using one of two pressure profiles as denoted in Figure 7. The injection pressure profiles can either be applied in the numerical model as a linearly increasing source function that starts from an initial pressure and is then followed by a shut-in period (for comparison with the analytical solution) or as a user specified profile in tabular form that may take the form of an experimentally determined injection pressure. In the numerical model for transient pore pressure diffusion, the measured wellhead injection pressure was replicated.

At the beginning of the calculation ($t = 0$) the initial condition in the reservoir nodes is set $= 0$ Pa. The shut-in time is denoted at $t = 400,000$ seconds (equivalent to ~111 hours); after this time no pressure source is applied and the pressure at the injection point is calculated from a natural boundary condition denoted by:

$$\frac{\partial p}{\partial t} = 6D\left(\frac{\partial^2 p}{\partial r^2}\right).$$

(3)

By numerically solving the hydrological model the subsurface pressure as a function of both time and distance from the injection point is obtained. Illustrations of calculated pressure profiles as a function of distance for different simulation times and as a function of simulation time for different distance from the injection point using the numerical approach are shown in Figures 8 and 9, "respectively". The profiles for the linearly increasing injection source indicate that the extent of pore
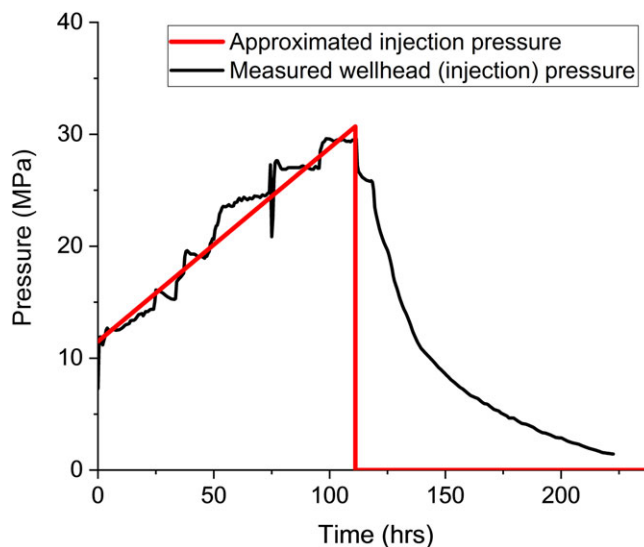

FIGURE 7 Approximated and measured injection pressure for the Basel EGS (Dinske, 2010; Häring et al., 2008)
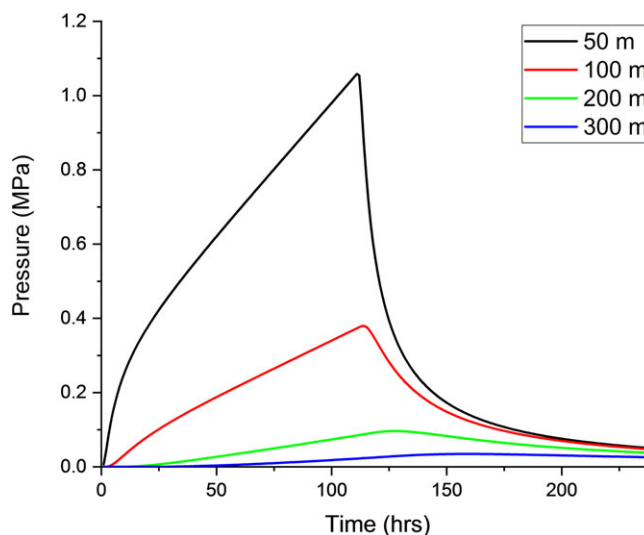

FIGURE 8 Pore pressure profiles from numerically solving the diffusion equation as a function of distance to source point
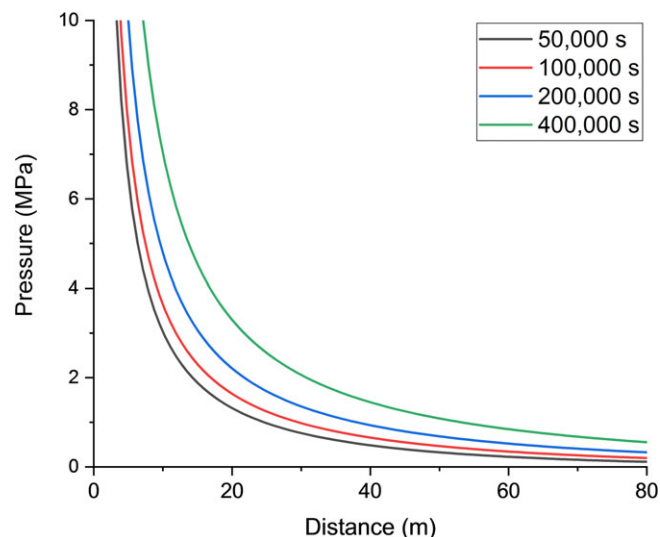
FIGURE 9 Pore pressure profiles from numerically solving the diffusion equation as a function of time. Injection stop time is at 400,000 seconds
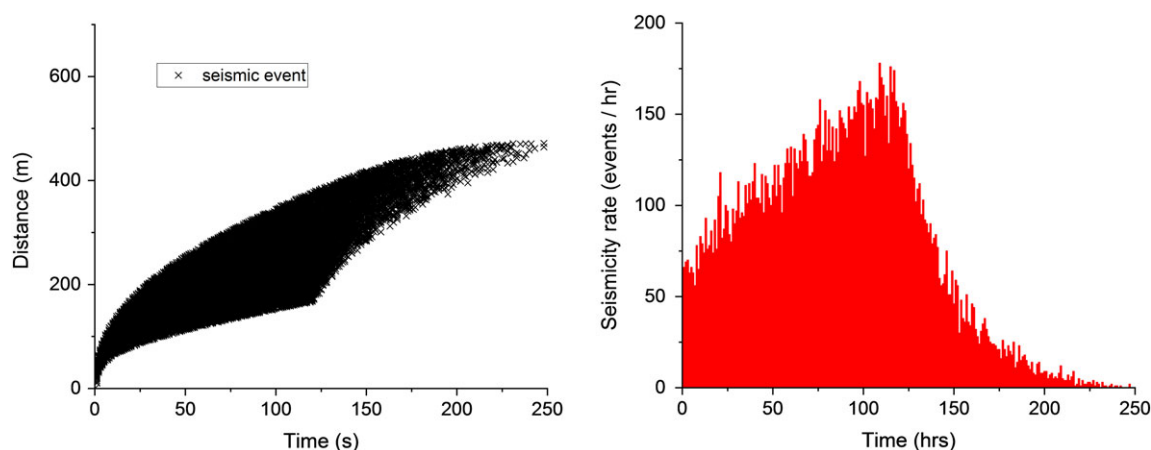

FIGURE 10 Simulated evolution of seismicity in a distance versus time plot (left) and a numerical seismicity rate plot (right) using the approach of Dinske (2010). During the simulation, 18,682 seismic events were recorded

pressure penetration is controlled in this model only by hydraulic diffusivity and the injection source characteristics. The magnitude of the pore pressure perturbation is impacted significantly by the injection pressure source, particularly at locations close to the source.

Once the pore pressure profiles are known, one attempts to predict the induced seismicity. Induced seismicity is generated using a simple geomechanical model, which assesses the impact of pore pressure perturbation on spatial stochastic distribution of preexisting fractures, with concentration 2.44×10^{-4} m^{-3} (Dinske, 2010). Each fracture is randomly assigned a critical stress parameter between the lower limit $Cmin = 9,600$ Pa and the upper limit $Cmax = 0.15$ MPa. These values are selected in an attempt to recreate the spatiotemporal behavior of seismicity observed at Basel. Once the pore pressure at each fracture's spatial location exceeds its critical stress parameter, a seismic event is recorded. Once one seismic event is recorded, no further events can occur in the same fracture. The results, shown in Figure 10 (right plot), illustrate the timing and distance from the injection location of the recorded events (*r-t* plot). The model, albeit simple, replicates qualitatively the *r-t* plots dataset from the Basel induced seismicity events (this model predicts 18,682 micro-earthquakes within a sphere of 500 m from the injection point, while ~13,500 events were recorded during the Basel stimulation). From the model, the seismicity rate, defined as the number of events per hour, can be generated (see left plot in Figure 10). The seismicity rate generally increases as the pore pressure in the reservoir increases. In some locations in the reservoir, the pore pressure can still increase for some time after the shut-in, which could cause induced seismicity. After a certain period post shut-in, the seismicity rate decays.

While the approach illustrated here provides a useful method for predicting the spatiotemporal evolution of seismicity during fluid injection, with the reservoir considered as homogenous, no attempt is made to describe the increase in reservoir permeability that will result during stimulation. In reality, rock stimulation will result in considerable changes to its permeability, which may be estimated as a function of reservoir pressure. Methods to model nonlinear pore-fluid pressure diffusion

associated with heterogeneously and time-dependent distributed permeability have been proposed (Hummel & Shapiro, 2013). Additionally, the diffusion approach implemented in the simple model described above may not be accurate for situations where a single planar hydraulic fracture acts as the conduit to fluid flow. Finally, the simple method described above does not provide information about the resulting magnitudes of the events. The prediction of seismic event magnitudes is challenging and no reliable methods currently exist for estimating the potential maximum induced seismic event at a location (StatesFirst, 2015). Because the magnitude of fluid injection induced seismic events is modeled to follow Gutenberg-Richter statistics (Shapiro, Dinske, & Kummerow, 2007), attempts can be made using geomechanics to predict the variation of *b*-value and stress drop that are observed during operations (Goertz-Allman & Wiemer, 2013), leading to magnitude estimations. Baisch et al. (2010) proposed an approach to predict event magnitudes by stress transfer across mechanically coupled rock patches. As another approach, knowledge of the rupture dynamics, could be used to predict seismic moment, which is described by:

$$M_0 = GAd, \tag{4}$$

where *G* is the shear modulus—a material property of the rock, *A* is the fault rupture area and *d* is the fault slip.; however, prediction of the average fault displacement is difficult. Empirical relationships between magnitude and fault dimensions for naturally occurring earthquakes larger than magnitude 5.0 have been developed by Wells and Coppersmith (1994) and may be used to estimate magnitude of potential-induced seismic events if fault size is known.

A further class of model relates to ground-motion prediction, which can be used to assess the impact of seismic events on local populations and infrastructure. Due consideration of the impact of model uncertainties on seismicity predictions is essential for adequate interpretation of results from such models. Real-time data obtained through seismic monitoring may be fed to statistical models for adaptive traffic light systems (see Mignan, Broccardo, Wiemer, & Giardini, 2017 for details of such systems). Such models are based on assessed thresholds which are updated on-the-fly as soon as new data becomes available.

9 | CONCLUSION

Geo-energy subsurface operations such as shale gas exploration and production, but also conventional oil and gas production, enhanced geothermal energy, carbon sequestration and others, including mining, could trigger-induced seismic events. Induced seismicity has been recognized for around a century but nowadays the risks associated with more recently emerging technologies such as hydraulic fracturing for shale production and EGS are on the increase. This review study was motivated by the need to provide a holistic perspective to risk management of induced seismicity that encompasses both technical and social aspects. Some examples of seismic events occurred over the past 15 years are briefly reviewed here, together with a discussion of the public and governmental responses.

Analysis of case study histories of induced seismic events indicates that the risk of damage or injury posed by induced seismicity in most cases of hydraulic fracturing are generally lower compared to those related to large scale waste water disposal and other industrial activities, but may depend on regional geology and natural seismicity. The possible mechanisms that could lead to induced seismic events are reviewed, together with typical approaches that are put in place to safeguard the environment, for example, the traffic light system. Emphasis is on the different thresholds that are implemented in different locations, as well as on the public acceptance and response to both the induced seismic events and the safety protocols implemented in various regions. The importance of monitoring, modeling and predicting induced seismicity is discussed, with emphasis on current technology for monitoring and on the necessary compromise between accuracy of model predictions and availability of representative data. It is recognized that induced seismicity poses a significant reputational risk for companies engaged in subsurface operations, with the potential to compromise their social license to operate and ultimately shutdown operations. Minimizing seismic risk should therefore be a high priority for operators.

In Europe, the regulatory framework that governs unconventional energy development is developing. In the United Kingdom, uncertainty remains in unconventional oil and gas development as to quantities of produced wastewater and regulations and mechanisms for treatment and reuse or disposal (O'Donnell, Gilfillan, Eldmann, & McDermott, 2018). Where reinjection of wastewater for disposal may be allowed in certain circumstances it would require careful regulation for the avoidance of induced seismicity. All fluid injection processes should require detailed seismic hazard assessments for imaging and characterizing faults prior to operations, with dedicated monitoring systems in addition to existing national seismic monitoring facilities. Traffic light systems should be used with carefully considered thresholds. For assessing the risks, monitoring the operations, and designing mitigation strategies using predictive models that can characterize the spatiotemporal evolution of induced seismicity would be extremely helpful. Some simple models are presented herein, and references are provided for recent developments in the sector. Ultimately, especially in areas with large population density, successful subsurface geo-energy operations require a social license to operate. Examples of best practice approaches show that maintaining a transparent

dialogue between operator and the public, while adhering to the regulatory processes can allow safe operations in an atmosphere of public acceptance.

ACKNOWLEDGMENTS

CONFLICT OF INTEREST

The authors have declared no conflicts of interest for this article.

RELATED WIREs ARTICLE

Public perceptions of hydraulic fracturing for shale gas and oil in the United States and Canada
Seismic event identification

REFERENCES

Albano, M., Polcari, M., Bignami, C., Moro, M., Saroli, M., & Stramondo, S. (2017). Did anthropogenic activities trigger the 3 April 2017 M^w 6.5 Botswana earthquake? *Remote Sensing*, *9*(10), 1028. https://doi.org/10.3390/rs9101028

Altmann, J. B. (2010). *Poroelastic effects in reservoir modelling.* (Doctoral thesis). Karlsruhe Institute of Technology). Retrieved from https://publikationen.bibliothek.kit.edu/1000021248

Andersson-Hudson, J., Knight, W., & Humphrey, M. (2016). Exploring support for shale gas extraction in the United Kingdom. *Energy Policy*, *98*, 582–589. https://doi.org/10.1016/j.enpol.2016.09.042

Atkinson, G. M., Eaton, D. W., Ghofrani, H., Walker, D., Cheadle, B., Schultz, R., … Kao, H. (2016). Hydraulic fracturing and induced seismicity in the Western Canada Sedimentary Basin. *Seismological Research Letters*, *87*, 631–647. https://doi.org/10.1785/0220150263

Bachmann, C. E., Wiemer, S., Goertz-Allman, B. P., & Woessner, J. (2012). Influence of pore-pressure on the event-size distribution of induced earthquakes. *Geophysical Research Letters*, *39*, L09302.

Baisch, S., Voros, R., Rothert, E., Stang, H., Jung, R., & Schellschmidt, R. (2010). A numerical model for fluid injection induced seismicity at Soult-Sous-Forets. *International Journal of Rock Mechanics and Mining Sciences*, *47*, 405–413. https://doi.org/10.1016/j.ijrmms.2009.10.001

Banks, E. (2006). *Catastrophic risk: Analysis and management*. Chichester, England: Wiley Finance.

Bendall, B., Love, D., Hough, P., Malavazos, M., Long, A., & Pepicelli, D. (2012, January 30–February 1). *Towards Understanding Induced Seismicity.* Paper in 37th Workshop on Geothermal Reservoir Engineering. Stanford University, Stanford, California, SGP-TR-194.

Bessason, B., Ólafsson, E. H., Gunnarsson, G., Flóvenz, Ó. G., Jakobsdóttir, S. S., Björnsson, S., & Árnadóttir, Th. (2012). *Work procedures due to induced seismicity in geothermal systems* (Report 2012–24). Reykjavík Energy, Reykjavík, Iceland (in Icelandic), 118 pp.

Bohnhoff, M., Malin, P., ter Heege, J., Delflandre, J. P., & Sicking, C. (2018). Suggested best practice for seismic monitoring and characterization of non-conventional reservoirs. *First Break*, *36*, 59–64.

Bommer, J. J., Crowley, H., & Pinho, R. (2015). A risk-mitigation approach to the management of induced seismicity. *Journal of Seismology*, *19*, 623–646. https://doi.org/10.1007/s10950-015-9478-z

Bommer, J. J., Oates, S., Cepeda, J. M., Lindolm, C., Bird, J., Torres, R., … Rivas, J. (2006). Control of hazard due to seismicity induced by a hot fractured rock geothermal project. *Engineering Geology*, *83*(4), 287–306. https://doi.org/10.1016/j.enggeo.2005.11.002

Byerlee, J. D. (1987). Friction of rocks. *Pure and Applied Geophysics*, *116*, 615–626.

Cesca, S., Dost, B., & Oth, A. (2013). Preface to the special issue "triggered and induced seismicity: Probabilities and discrimination". *Journal of Seismology*, *17*, 1–4.

Cesca, S., & Grigoli, F. (2015). Full waveforms seismological advances for microseismic monitoring. *Advances in Geophysics*, *56*, 169–228. https://doi.org/10.1016/bs.agph.2014.12.002

Clarke, H., Eisner, L., Styles, P., & Turner, P. (2014). Felt seismicity associated with shale gas hydraulic fracturing: The first documented example in Europe. *Geophysical Research Letters*, *41*, 8308–8314. https://doi.org/10.1002/2014GL062047

Davey, E. (2012, December 13). *Written ministerial statement by Edward Davey: Exploration for shale gas.* Retrieved from https://www.gov.uk/government/speeches/written-ministerial-statement-by-edward-davey-exploration-for-shale-gas

Davies, R. J., Foulger, G., Bindley, A., & Styles, P. (2013). Induced seismicity and hydraulic fracturing for the recovery of hydrocarbons. *Marine and Petroleum Geology*, *45*, 171–185. https://doi.org/10.1016/j.marpetgeo.2013.03.016

de Pater, C. J., & Baisch, S. (2011). *Geomechanical study of Bowland shale seismicity* (Synthesis Report, Nov. 2). Cuadrilla Resources, Staffordshire, UK.

Deng, K., Zhou, S., Wang, R., Robinson, R., Zhao, C., & Cheng, W. (2010). Evidence that the 2008 M_W 7.9 Wenchuan earthquake could not have been induced by the Zipingpu reservoir. *Bulletin of the Seismological Society of America*, *100*(5B), 2805–2814. https://doi.org/10.1785/0120090222

Dinske, C. (2010). *Interpretation of fluid-induced seismicity at geothermal and hydrocarbon reservoirs of basel and cotton valley.* (Doctoral Thesis). Free University of Berlin. Retrieved from http://www.diss.fu-berlin.de/diss/receive/FUDISS_thesis_000000023148

EADD (Environment Agency Decision Document). (2014). EPR/AB3101MW.

Edwards, B., & Douglas, J. (2014). Magnitude scaling of induced earthquakes. *Geothermics*, *52*, 132–139. https://doi.org/10.1016/j.geothermics.2013.09.012

EIA (Energy Information Administration) & ARI (Advanced Resources International). (2013). *World shale gas and shale oil resource assessment*. Washington, DC: EIA and ARI. Retrieved from http://www.adv-res.com/pdf/A_EIA_ARI_2013%20World%20Shale%20Gas%20and%20Shale%20Oil%20Resource%20Assessment.pdf

Ellsworth, W. L. (2013). Injection-induced earthquakes. *Science*, *341*, 1225942. https://doi.org/10.1126/science.1225942

Fault Slip Potential. (n.d.). Retrieved from https://scits.stanford.edu/fault-slip-potential

Fischer, T., & Guest, A. (2011). Shear and tensile earthquakes caused by fluid injection. *Geophysical Research Letters*, *38*, L05307. https://doi.org/10.1029/2010GL045447

Foulger, G. R., Wilson, M. P., Gluyas, J. G., Julian, B. R., & Davies, R. J. (2018). Global review of human-induced earthquakes. *Earth-Science Reviews*, *178*, 438–514. https://doi.org/10.1016/j.earscirev.2017.07.008

Ge, S., Liu, M., Lu, M., Godt, J. W., & Luo, G. (2009). Did the Zipingpu reservoir trigger the 2008 Wenchuan earthquake? *Geophysical Research Letters*, *36*, L20315. https://doi.org/10.1029/2009GL040349

Giardini, D. (2009). Geothermal quake risks must be faced. *Nature*, *462*, 848–849. https://doi.org/10.1038/462848a

Gischig, V., Wiemer, S., & Alcolea, A. (2014). Balancing reservoir creation and seismic hazard in enhanced geothermal systems. *Geophysical Journal International*, *198*, 1585–1598. https://doi.org/10.1093/gji/ggu221

Gischig, V. S., & Wiemer, S. (2013). A stochastic model for induced seismicity based on non-linear pressure diffusion and irreversible permeability enhancement. *Geophysical Journal International*, *194*(2), 1229–1249. https://doi.org/10.1093/gji/ggt164

Goertz-Allman, B. P., & Wiemer, S. (2013). Geomechanical modelling of induced seismicity source parameters and implications for seismic hazard assessment. *Geophysics*, *78*, KS25–KS39. https://doi.org/10.1190/geo2012-0102.1

Graham, J. D., Rupp, J. A., & Schenk, O. (2015). Unconventional gas development in the USA: Exploring risk perception issues. *Risk Analysis*, *35*(10), 1770–1788. https://doi.org/10.1111/risa.12512

Green, C. A., Styles, P., & Baptie, B. J. (2012). *Preese hall shale gas fracturing: Review and recommendations for induced seismic mitigation*. London, England: Department of Energy and Climate Change.

Grigoli, F., Cesca, S., Priolo, E., Rinaldi, A. P., Clinton, J. F., Stabile, T. A., … Dahm, T. (2017). Current challenges in monitoring, discriminating and management of induced seismicity related to underground industrial activities: A European perspective. *Reviews of Geophysics*, *55*, 310–340. https://doi.org/10.1002/2016RG000542

Grigoli, F., Cesca, S., Rinaldi, A. P., Manconi, A., López-Comino, Clinton, J. F., … Wiemar, S. (2018). The November 2017 MW 5.5 Pohang earthquake: A possible case of induced seismicity in South Korea. *Science*, *360*, 1003–1006. https://doi.org/10.1126/science.aat2010

Grigoli, F., Scarabello, L., Böse, M., Weber, B., & Wiemer, S. (2018). Pick- and waveform-based techniques for real-time detection of induced seismicity. *Geophysical Journal International*, *213*, 868–884. https://doi.org/10.1093/gji/ggy019

Häring, M. O., Schanz, U., Ladner, F., & Dyer, B. C. (2008). Characterisation of the Basel 1 enhanced geothermal system. *Geothermics*, *37*, 489–495. https://doi.org/10.1016/j.geothermics.2008.06.002

Howell, B. F., Jr. (1981). On the saturation of earthquake magnitude. *Bulletin of the Seismological Society of America*, *71*, 1401–1422.

Hummel, N., & Shapiro, S. A. (2013). Nonlinear diffusion-based interpretation of induced microseismicity: A Barnett shale hydraulic fracturing case study. *Geophysics*, *78*, B211–B226. https://doi.org/10.1190/geo2012-0242.1

Induced Seismicity. (2017, October 13). Retrieved from https://earthquake.usgs.gov/research/induced/

Juncu, D., Árnadóttir, T., Geirsson, H., Guðmundsson, G. B., Lund, B., Gunnarsson, G., … Michalczewska, K. (2018). *Journal of Volcanology and Geothermal Research*. https://doi.org/10.1016/j.jvolgeores.2018.03.019

Kao, H., Eaton, D.W., Atkinson, G.M., Maxwell, S., & Babaie Mahani, A. (2016). *Technical Meeting on the Traffic Light Protocols (TLP) for induced Seismicity: Summary and Recommendations*. Geological Survey of Canada, Open File 8075. doi:https://doi.org/10.4095/299002

Keranen, K. W., & Weingarten, M. (2018). Induced seismicity. *Annual Review of Earth and Planetary*, *46*, 149–174. https://doi.org/10.1146/annurev-earth-082517-010054

Kim, K.-H., Ree, J.-H., Kim, Y., Kim, S., Kang, S. Y., & Seo, W. (2018). Assessing whether the 2017 M^W 5.4 Pohang earthquake in South Korea was an induced event. *Science*, *360*, 1007–1009. https://doi.org/10.1126/science.aat6081

Klose, C. D. (2010). Human-triggered earthquakes and their impacts on human security, achieving environmental security: Ecosystem services and human welfare. In P. H. Liotta, W.G. Kepner, J.M. Lancaster & D.A. Mouat. (Eds.), *NATO science for peace and security series—E: Human and societal dyanamics* (Vol. 69, pp. 13–19). Amsterdam, Netherlands: IOS Press.

Kraft, T., & Deichmann, N. (2014). High-precision relocation and focal mechanism of the injection-induced seismicity at the Basel EGS. *Geothermics*, *52*, 59–73. https://doi.org/10.1029/2012GL051480

Langenbruch, C., & Zoback, M. D. (2016). How will induced seismicity in Oklahoma respond to decreased saltwater injection rates? *Science Advances*, *2*(11), e1601542. https://doi.org/10.1126/sciadv.1601542

Lei, X., Huang, D., Su, J., Wang, X., Wang, H., Guo, X., & Fu, H. (2017). Fault reactivation and earthquakes with magnitudes of up to mw 4.7 induced by shale-gas hydraulic fracturing in Sichuan Basin, China. *Scientific Reports*, *7*, 7971. https://doi.org/10.1038/s41598-017-08557-y

Li, T., Zhou, X., & Li, H. (2013, May 13–16). *Environmental Impacts of Shale Gas Development in China and Recommendations on Management of their Environmental Impact Assessment*. Paper presented at the 33rd Annual Meeting of the International Association for Impact Assessment, Calgary.

Majer, E., Nelson, J., Robertson-Tai, A., Savy, J., & Wong, I. (2011), *Protocol for addressing induced seismicity associated with enhanced geothermal systems*. Retrieved from http:ww1.eere.energy.gov/geothermal/pdfs/egs-is-protocol-final-draft-20110531.pdf

Majer, E. L., Baria, R., Stark, M., Oates, S., Bommer, J., Smith, B., & Asanuma, H. (2007). Induced seismicity associated with enhanced geothermal systems. *Geothermics*, *36*, 185–222. https://doi.org/10.1016/j.geothermics.2007.03.003

Maxwell, S. C. (2013). Unintentional seismicity induced by hydraulic fracturing. *GSEG Recorder,* October, 40–49.

McComas, K. A., Lu, H., Keranen, K. M., Furtney, M. A., & Song, H. (2016). Public perceptions and acceptance of induced earthquakes related to energy development. *Energy Policy*, *99*, 27–32. https://doi.org/10.1016/j.enpol.2016.09.026

McGarr, A. (2014). Maximum magnitude earthquakes induced by fluid injection. *Journal of Geophysical Research. Solid Earth*, *119*, 1008–1019.

McGarr, A., Simpson, D., & Seeber, L. (2002). Case histories of induced and triggered seismicity. In W. Lee, P. Jennings, C. Kisslinger, & H. Kanamori (Eds.), *International handbook of earthquake and engineering seismology* (pp. 647–661). Waltham, MA: Academic Press.

Mertz, E., & Ramsay, C. (2016). St. Albert feels tremors from earthquake near Fox Creek. *Global News*, 12 January [Online]. Retrieved from https://globalnews.ca/news/2449048/earthquake-reported-in-northern-alberta-town/

Mignan, A., Broccardo, M., Wiemer, S., & Giardini, D. (2017). Induced seismicity closed-form traffic light system for actuarial decision-making during deep fluid injections. *Scientific Reports*, *7*, 13607.

Muntendam-Bos, A. G., Roest, J. P. A., & de Waal, H. A. (2017). The effect of imposed production measures on gas extraction induced seismic risk. *Netherlands Journal of Geosciences*, *96*(5), s271–s278. https://doi.org/10.1017/njg.2017.29

O'Donnell, M. C., Gilfillan, S. M. V., Eldmann, K., & McDermott, C. I. (2018). Wastewater from hydraulic fracturing in the UK: Assessing the viability and cost of management. *Environmental Science: Water Research & Technology*, *4*, 325–335. https://doi.org/10.1039/C7EW00474E

O'Hara, S., Humphrey, M., Andersson-Hudson, J., & KnightPublic, W. (2015). *Perception of shale gas extraction in the UK: Two years on from the Balcombe protests. Report of the Nottingham tracker survey on public perception of shale gas extraction*. Nottingham, England: University of Nottingham.

Park, S., Xie, L., Kim, K., Kwon, S., Min, K., Choi, J., … Song, Y. (2017). First hydraulic stimulation in fractured geothermal reservoir in Pohang PX-2 well. *Procedia Engineering*, *191*, 829–837. https://doi.org/10.1016/j.proeng.2017.05.250

Pesicek, J. D., Child, D., Artman, B., & Cieślik, K. (2014). Picking versus stacking in a modern microearthquake location: Comparison of results from a surface passive seismic monitoring array in Oklahoma. *Geophysics*, *79*(6), KS61–KS68. https://doi.org/10.1190/geo2013-0404.1

Petersen, M. D., Mueller, C. S., Moschetti, M. P., Hoover, S. M., Rukstales, K. S., McNamara, D. E., … Cochran, E. S. (2018). 2018 one-year seismic hazard forecast for the central and eastern United States from induced and natural earthquakes. *Seismological Research Letters*, *89*, 1049–1061. https://doi.org/10.1785/0220180005

Rutqvist, J. (2011). Status of the TOUGH-FLAC simulator and recent applications related to coupled fluid flow and crustal deformations. *Computers & Geosciences*, *37*, 739–750. https://doi.org/10.1016/j.cageo.2010.08.006

Schultz, R., Atkinson, G., Eaton, D. W., Gu, Y. G., & Kao, H. (2018). Hydraulic fracturing volume is associated with induced earthquake productivity in the Duvernay play. *Science*, *359*, 304–308. https://doi.org/10.1126/science.aao0159

Schultz, R., Wang, R., Gu, Y. J., Haug, K., & Atkinson, G. (2017). A seismological overview of the induced earthquakes in the Duvernay play near Fox Creek, Alberta. *Journal of Geophysical Research. Solid Earth*, *122*, 492–505. https://doi.org/10.1002/2016JB013570

Segall, P., & Lu, S. (2015). Injection-induced seismicity: Poroelastic and earthquake nucleation effects. *Journal of Geophysical Research. Solid Earth*, *120*, 5082–5103. https://doi.org/10.1002/2015JB012060

Shapiro, S. A., Audigane, P., & Royer, J. J. (1999). Large-scale in situ permeability tensor of rocks from induced microseismicity. *Geophysical Journal International*, *137*, 207–213. https://doi.org/10.1046/j.1365-246x.1999.00781.x

Shapiro, S. A., & Dinske, C. (2009). Fluid-induced seismicity: Pressure diffusion and hydraulic fracturing. *Geophysical Prospecting*, *57*, 301–310. https://doi.org/10.1111/j.1365-2478.2008.00770.x

Shapiro, S. A., Dinske, C., & Kummerow, J. (2007). Probability of a given-magnitude earthquake induced by a fluid injection. *Geophysical Research Letters*, *34*, 22. https://doi.org/10.1029/2007GL031615

StatesFirst. (2015). *Potential injection-induced seismicity associated with oil & gas development: A primer on technical and regulatory considerations informing risk management and mitigation*. StatesFirst induced seismicity by injection work group (ISWG), Interstate Oil and Gas Compact Commission and the Ground Water Protection Council.

Stork, A. L., Verdon, J. P., & Kendall, J. M. (2014). Assessing the effect of velocity model accuracy on microseismic interpretation at the in Salah carbon capture and storage site. *Energy Procedia*, *63*, 4385–4393. https://doi.org/10.1016/j.egypro.2014.11.473

Suckale, J., & Grünthal, G. (2009). Probabilistic Seismic Hazard Model for Vanuatu. *Bulletin of the Seismological Society of America*, *99*(4), 2108–2126.

Tao, W., Masterlark, T., Shen, Z. K., & Ronchin, E. (2015). Impoundment of the Zipingpu reservoir and triggering of the 2008 M_W 7.9 Wenchuan earthquake, China. *Journal of Geophysical Research. Solid Earth*, *120*, 7033–7047. https://doi.org/10.1002/2014JB011766

TerHeege, J. (2016). *Recent shale developments in the Netherlands*. Presentation at The Shale Exchange, Pittsburgh, USA, 10 October. Retrieved from http://www.m4shalegas.eu/downloads/J.%20TerHeege%20-%20M4ShaleGas%20-%20Recent%20shale%20developments%20in%20the%20Netherlands%20-%2010-2016.pdf

Trutnevyte, E., & Ejderyan, O. (2017). Managing geoenergy-induced seismicity with society. *Journal of Risk Research*, 1–8. https://doi.org/10.1080/13669877.2017.1304979

Urban, K. (2017, April 23–28). *Reporting from the Iceland deep drilling project*. Paper presented at 19th EGU general assembly, EGU2017. Vienna, Austria.

van der Voort, N., & Vanclay, F. (2015). Social impacts of earthquakes caused by gas extraction in the province of Groningen, the Netherlands. *Environmental Impact Assessment Review*, *50*, 1–15. https://doi.org/10.1016/j.eiar.2014.08.008

van Thienen-Visser, K., & Breunese, J. N. (2015). Induced seismicity of the Groningen gas field: History and recent developments. *The Leading Edge*, *34*, 664–671. https://doi.org/10.1190/tle34060664.1

Verdon, J. P., Kendall, J. M., Hicks, S. P., & Hill, P. (2017). Using beamforming to maximise the detection capability of small sparse seismometer arrays deployed to monitor oil field activities. *Geophysical Prospecting*, *65*, 1582–1596. https://doi.org/10.1111/1365-2478.12498

Vlek, C. (2018). Induced earthquakes from long-term gas extraction in Groningen, the Netherlands: Statistical analysis and prognosis for acceptable-risk regulation. *Risk Analysis*, *38*, 1455–1473. https://doi.org/10.1111/risa.12967

Wald, D. J., Quitoriano, V., Heaton, T. H., & Kanamori, H. (1999). Relationship between peak ground acceleration, peak ground velocity, and modified Mercalli intensity in California. *Earthquake Spectra*, *15*(3), 557–564. https://doi.org/10.1193/1.1586058

Wald, D. J., Worden, C. B., Lin, K. W., & Pankow, K. (2005). ShakeMap manual: technical manual, user's guide, and software guide. U. S. Geological Survey, Techniques and Methods 12-A1, 132 pp. http://pubs.usgs.gov/tm/2005/12A01/

Wallquist, L., Visschers, V. H. M., & Siegrist, M. (2009). Lay concepts on CCS deployment in Switzerland based on qualitative interviews. *International Journal of Greenhouse Gas*, *3*, 652–657. https://doi.org/10.1016/j.ijggc.2009.03.005

Warpinski, N. R., Du, J., & Zimmer, U. (2012). Measurements of hydraulic-fracture-induced seismicity in gas shales. *SPE*, 151597. https://doi.org/10.2118/151597-MS

Warpinski, N. R., Mayerhofer, M., Agarwal, K., & Du, J. (2013). Hydraulic-fracture geomechanics and microseismic-source mechanism. *SPE Journal*, *18*(4) 766–780. https://doi.org/10.2118/158935-PA

Weingarten, M., Ge, S., Godt, J. W., Bekins, B. A., & Rubinstein, J. L. (2015). High-rate injection is associated with the increase in U.S. mid-continent seismicity. *Science*, *348*, 1336–1340. https://doi.org/10.1126/science.aab1345

Wells, D. L., & Coppersmith, K. J. (1994). New empirical relationships among magnitude, rupture length, rupture width, rupture area, and surface displacement. *Bulletin of the Seismological Society of America*, *84*, 974–1002.

Wiemer, S., Kraft, T., Trutnevyte, E., & Phillipe, R. (2017). *"Good practice" guide for managing induced seismicity in deep geothermal energy projects in Switzerland* (p. 2017). Zurich, Switzerland: Swiss Seismological Service. https://doi.org/10.12686/a5

Williams, L., Macnaghten, P., Davies, R., & Curtis, S. (2017). Framing 'fracking': Exploring public perceptions of hydraulic fracturing in the United Kingdom. *Public Understanding of Science*, *26*, 89–104. https://doi.org/10.1177/0963662515595159

White, J. A., & Foxall, W. (2016). Assessing induced seismicity risk at CO2 storage projects: Recent progress and remaining challenges. *International Journal of Greenhouse Gas Control*, *49*, 413–424. https://doi.org/10.1016/j.iggc.2016.03.021

Zhang, H., Eaton, D. W., Li, G., Liu, Y., & Harrington, R. M. (2016). Discriminating induced seismicity from natural earthquakes using moment tensors and source spectra. *Journal of Geophysical Research: Solid Earth*, *121*, 972–993. https://doi.org/10.1002/2015JB012603